Mechanical Systems and Signal Processing 36 (2013) 182–192

Contents lists available at SciVerse ScienceDirect

Mechanical Systems and Signal Processing

journal homepage: www.elsevier.com/locate/ymssp

A simple fuzzy system for modelling of both rate-independent and rate-dependent hysteresis in piezoelectric actuators

Pengzhi Li*, Feng Yan, Chuan Ge, Xueliang Wang, Lisong Xu, Jialiang Guo, Peiyue Li

State Key Laboratory of Applied Optics, Changchun Institute of Optics, Fine Mechanics and Physics, Chinese Academy of Sciences, Changchun 130033, China

ARTICLE INFO

Article history:
Received 21 March 2012
Received in revised form
8 September 2012
Accepted 1 October 2012
Available online 27 October 2012

Keywords:
Fuzzy system
Rate-independent
Rate-dependent
Hysteresis
Piezoelectric actuator
T–S

ABSTRACT

In this paper, a novel fuzzy system based method for modelling both rate-independent and rate-dependent hysteresis in the piezoelectric actuator is proposed. First, the partial Takagi–Sugeno (T–S) fuzzy rule is designed. The antecedent structure of the fuzzy system is identified through uniform partition of its input variable. Then, the parameters of the consequent structure are optimized via the recursive least squares (RLS) algorithm. The modelling method is simple to implement and highly efficient to compute. Experimental results show that the proposed method is efficient to model both rate-independent and rate-dependent hysteresis. Based on the inverse of the developed model, feed-forward hysteresis compensation experiments at the frequencies of 50 Hz and 100 Hz are also conducted with the hysteresis effects being obviously reduced. The major contribution of this paper is that the inverse of the model can be analytically computed and the method can be applied to the case of real-time on-line modelling.

1. Introduction

Hysteresis is a peculiar feature widely existing in the magnetic and ferroelectric materials. Piezoelectric ceramics is one kind of ferroelectric materials. Ferroelectric materials are crystals which are polar without an electric field being applied. This state is termed spontaneous polarization. By applying a strong electric field, the spontaneous polarization is reoriented to the saturation polarization. This produces a residual polarization parallel to the direction of the field, and then the material becomes piezoelectric [1]. The lead–zirconate–titanate ceramics (PZT) mainly in use today are $PbTiO_3$–$PbZrO_3$ compounds. The piezoelectric actuator, which is widely used in nanotechnology, ultra-precise machining, biotechnology and optical inspection, consists of piezoelectric ceramics. However, the intrinsic non-linear and multi-valued hysteresis in the piezoelectric actuator has the potential to cause inaccuracy or instability of its applied system. As shown in Fig. 1, the hysteresis is often characterized by non-linearity and rate-dependence. Non-linearity means that the same input voltage has different output displacements during the period of voltage increase and decrease. It implies voltage–displacement hysteresis curve is not one–one mapping. Besides, rate-dependence indicates that the frequency of input voltage has influence on not only the shape but also the orientation of hysteresis curve.

In the last decade, many models such as Preisach model [2,3], Prandtl–Ishlinskii (PI) model [4–6], Maxwell slip model [7], Duhem model [5] and Jiles–Atherton model [8] are presented mainly for rate-independent hysteresis. As to rate-dependent hysteresis, Ang [9] and Janaideh [10] proposed two modified PI models combining the density functions of time

* Corresponding author. Tel.: +86 431 8617 6905; fax: +86 431 8670 8158.
E-mail address: kindrobot@163.com (P. Li).

0888-3270/$ - see front matter © 2012 Elsevier Ltd. All rights reserved.
http://dx.doi.org/10.1016/j.ymssp.2012.10.004

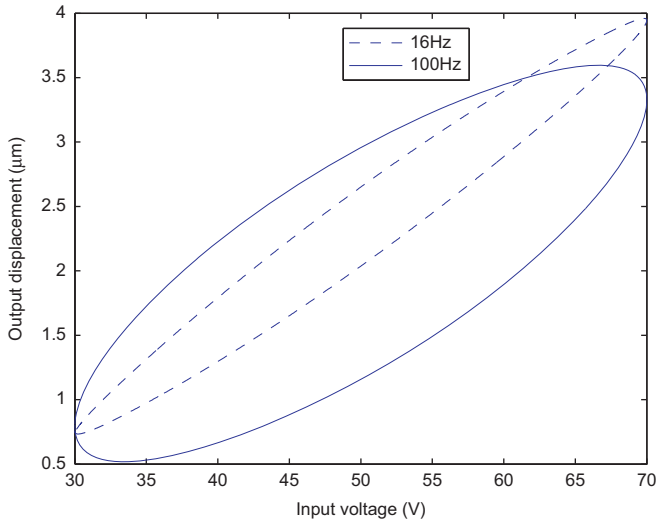

Fig. 1. Hysteresis curve of the piezoelectric actuator.

rate of input. Neural networks were applied to the approximation of the rate-independent or rate-dependent hysteresis based on the expanded input space [11–13]. An elliptical mathematical model was developed to describe the rate-dependent hysteresis effects in piezoelectric actuators [14]. An improved on-line least squares support vector machines based modelling method was presented for identifying rate-dependent hysteresis non-linearity in giant magnetostrictive actuator [15]. Recently, fuzzy system has been broadly utilized in many fields such as expert systems, signal processing, non-linear modelling and especially automatic control [16–19]. The authors' of the former paper adopted first-order Takagi–Sugeno (T–S) [20] fuzzy system to model hysteresis in piezoelectric actuators by introducing the nearest neighbour and super radius concepts [21]. The adaptive network fuzzy inference system was used to model the non-linear dynamic magnetic hysteresis and vector hysteresis [22,23]. The fuzzy subtractive clustering approach was developed for modelling shape memory alloy and airfoil hysteresis [24]. A sliding mode estimator was designed to estimate the unmeasured hysteresis output of the piezoelectric system [25]. However, these fuzzy hysteresis models above mainly focused on off-line modelling and there were no further consideration or development of the analytical inverse of the model. This paper proposes a simple T–S fuzzy system based model for both rate-independent and rate-dependent hysteresis. It uses uniform partition and recursive least squares (RLS) algorithm for identification and optimization. The inverse of the model can be analytically obtained and the method can be applied for on-linemodelling. Experimental results demonstrate its efficiency of modelling and inverse-based feed-forward control.

2. Fuzzy system for hysteresis

Fuzzy system is based on knowledge bases or IF–THEN fuzzy rules. Besides, it is also a multiple-input single-output mapping from a real-valued vector to a real-valued scalar and there exists precise analytic formulas of the mapping. Generally, a fuzzy system such as Mamdani-type [26] is composed of a fuzzifier, fuzzy rule base, fuzzy inference engine and defuzzifier, shown in Fig. 2(a). The fuzzifier transforms input real-valued variables to fuzzy sets. The fuzzy rule base can be viewed as sets of many fuzzy IF–THEN rules. The fuzzy inference engine adopts individual-rule or composition based inference method to map fuzzy sets in the input universe of discourse $U \subset R^n$ to ones in the output universe of discourse $Y \subset R$ based on some fuzzy logic. T–S fuzzy system has real-valued input and output variables, thus without the fuzzifier and defuzzifier, shown in Fig. 2(b). It consists of some piecewise linear systems and is especially proper for modelling non-linear systems. Hence we choose it to model the hysteresis in the piezoelectric actuator.

Consider a discrete-time system with hysteresis. The T–S fuzzy system has the following form of partial fuzzy rules:

$$R^l\text{: IF } y(k) \text{ is } A^l$$
$$\text{THEN } y(k+1) = q_{l1}y(k) + q_{l2}u(k) + q_{l3}, \quad l = 1, \ldots, L \tag{1}$$

where $y(k) = y(kT_s) = y_k$, $u(k) = u(kT_s) = u_k$ are the output and input of the system with hysteresis at the time instant kT_s respectively, T_s is the sampling period, q_{l1}, q_{l2},q_{l3} are real-valued parameters of the consequent structure, and L is the number of fuzzy rules.

The fuzzy set A^l is designed with Gaussian membership function $\mu_{A^l}(y_k)$ defined by

$$\mu_{A^l}(y_k) = \exp(-(y_k - c_l)^2/2(\sigma_l)^2) \tag{2}$$

where c_l,σ_l are the parameters of the membership function in the antecedent structure.

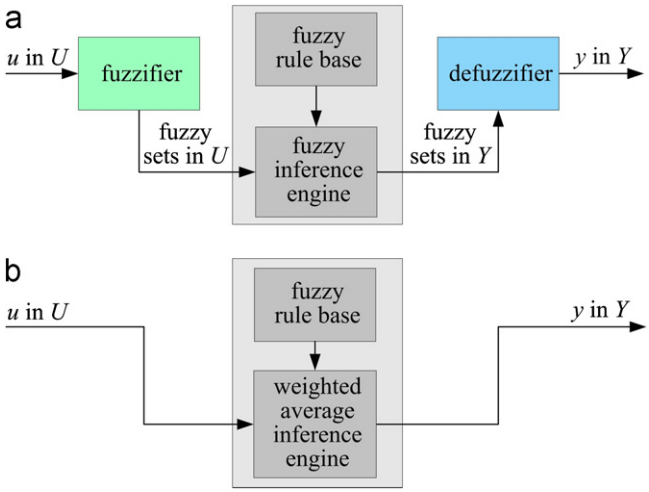

Fig. 2. Block diagram of fuzzy system: (a) Mamdani-type and (b) T–S type.

In fact, the 'partial' fuzzy rule of Eq. (1) is equivalent to the following one:

R^l: IF $y(k)$ is A^l and $u(k)$ is I^l

THEN $y(k+1) = q_{l1}y(k) + q_{l2}u(k) + q_{l3}, \quad l = 1, \ldots, L$

where I^l is a fuzzy set with the membership function $\mu_{I^l}(u_k) = 1$. The reasons for such design lie in two aspects. One is the simplicity of the antecedent parameters identification of the fuzzy system without considering u_k. The other is the inverse of the model that can be analytically obtained without u_k in the antecedent of fuzzy rule.

The fuzzy basis function (FBF), which can also be referred as weighted firing strength, is given by

$$p^l(y_k) = \frac{\mu_{A^l}(y_k)}{\sum_{l=1}^{L}(\mu_{A^l}(y_k))} \tag{3}$$

Finally, the weighted average output $\hat{y}_{k+1}$ of the fuzzy system is

$$\hat{y}_{k+1} = \sum_{l=1}^{L}(p^l(y_k)(q_{l1}y(k) + q_{l2}u(k) + q_{l3})) \tag{4}$$

Let the consequent parameters vector $\mathbf{q}_l \in R^{3\times 1}$ be $\mathbf{q}_l = [q_{l1}, q_{l2}, q_{l3}]^T$ and the extended input vector $\tilde{\mathbf{u}}_k \in R^{3\times 1}$ be $\tilde{\mathbf{u}}_k = [y_k, u_k, 1]^T$, then $\hat{y}_{k+1}$ of Eq. (4) can be rewritten as

$$\hat{y}_{k+1} = \sum_{l=1}^{L}(p^l(y_k)(\mathbf{q}_l^T \cdot \tilde{\mathbf{u}}_k)) \tag{5}$$

3. Identification and modelling

Hysteresis in the piezoelectric actuator is a multi-valued mapping and non-linear phenomenon. In order to solve the problem of multi-valued mapping, here we use extended input variable to model the hysteresis. Suppose we have sampled N pairs of experimental data $(y_k, u_k) = (y(k), u(k))$, $k = 1, \ldots, N$. Identification of the fuzzy system includes identification of its antecedent and consequent parameters.

As to antecedent parameters c_l, σ_l, $l = 1, \ldots, L$, due to the partial fuzzy rule structure, we can simply partition the input y_k variable uniformly. Suppose numerical range of y_k, $k = 1, \ldots, N$ is $[y_{min}, y_{max}]$, then

$$c_l = y_{min} + (y_{max} - y_{min})(l-1)/(L-1), \quad l = 1, \ldots, L \tag{6}$$

$$\sigma_1 = \sigma_2 = \cdots = \sigma_L = (y_{max} - y_{min})/(L-1) \tag{7}$$

Here we have obtained the antecedent structure of the fuzzy system; that is to say, fuzzy sets $A^l, l = 1, \ldots, L$ are known, illustrated as Fig. 3. The fuzzy sets are normal, complete and consistent. This uniform partition method is less complicated and more easily computed than subtractive and fuzzy c-mean clustering. Besides, it can be applied on-line.

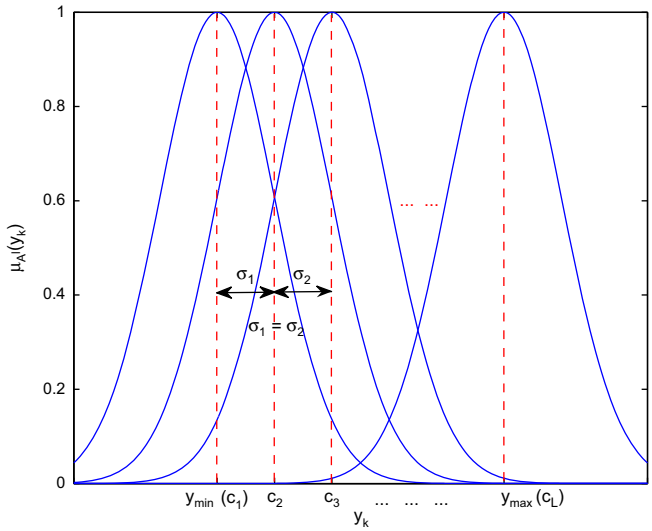

Fig. 3. Uniform partition of y_k in the antecedent structure of fuzzy system.

Next, we optimize the consequent parameters $\mathbf{q}_l, l=1,\ldots,L$ by using RLS algorithm. The performance criterion is chosen as

$$J=\frac{1}{2}\sum_{k=1}^{N}(e_m(k+1))^2=\frac{1}{2}\sum_{k=1}^{N}(y(k+1)-\hat{y}_{k+1})^2 \tag{8}$$

Expand $\hat{y}_{k+1}$ of Eq. (5) as

$$\hat{y}_{k+1}=p^1(y_k)\tilde{\mathbf{u}}_k^T\cdot\mathbf{q}_1+p^2(y_k)\tilde{\mathbf{u}}_k^T\cdot\mathbf{q}_2+\cdots+p^L(y_k)\tilde{\mathbf{u}}_k^T\cdot\mathbf{q}_L \tag{9}$$

Let $\overline{\mathbf{u}}_k\in R^{(3L)\times 1}$ be $\overline{\mathbf{u}}_k=[p^1(y_k)\tilde{\mathbf{u}}_k^T,p^2(y_k)\tilde{\mathbf{u}}_k^T,\ldots,p^L(y_k)\tilde{\mathbf{u}}_k^T]^T$ and $\mathbf{q}\in R^{(3L)\times 1}$ be $\mathbf{q}=[\mathbf{q}_1^T,\mathbf{q}_2^T,\ldots,\mathbf{q}_L^T,]^T$, then RLS algorithm at each time instant $k=1,2,\ldots,N$ can be written as

$$\begin{aligned}\mathbf{q}(k)&=\mathbf{q}(k-1)+\mathbf{K}(k)(y(k+1)-\overline{\mathbf{u}}_k^T\cdot\mathbf{q}(k-1))\\ \mathbf{K}(k)&=(\mathbf{P}(k-1)\overline{\mathbf{u}}_k)/(\lambda+\overline{\mathbf{u}}_k^T\mathbf{P}(k-1)\overline{\mathbf{u}}_k)\\ \mathbf{P}(k)&=\lambda^{-1}(\mathbf{I}-\mathbf{K}(k)\overline{\mathbf{u}}_k^T)\mathbf{P}(k-1)\end{aligned} \tag{10}$$

where $\mathbf{K}\in R^{(3L)\times 1}, \mathbf{P}\in R^{(3L)\times(3L)}, \mathbf{I}\in R^{(3L)\times(3L)}$ is an identity matrix and $\lambda\in(0,1]$ is the forgetting factor. The initial parameters can be chosen as $\mathbf{P}(0)=\alpha\mathbf{I}$ and $\mathbf{q}(0)=\varepsilon[1,1,\ldots]^T$ respectively, where α is a big positive constant value and ε is a small positive constant or zero value. The RLS algorithm is more efficient in computation and can be easily applied on-line for systems with volatile characteristics.

At last, the process of identification of the fuzzy system and modelling of hysteresis in the piezoelectric actuator is summarized as

Known: N pairs of experimental data $(y(k), u(k))$, $k=1,\ldots,N$.

Step 1. Calculate the numerical range $[y_{min},y_{max}]$ of $y_k, k=1,\ldots,N$.
Step 2. Choose the value L of the number of fuzzy rules.
Step 3. Use Eqs. (6), (7) and (2) to obtain fuzzy rules and membership functions.
Step 4. Choose the values λ, α and ε.
Step 5. Use Eqs. (3) and (10) to obtain the consequent parameters $\mathbf{q}$.
Step 6. The fuzzy system of Eq. (1) is achieved, then use Eq. (3) and (9) to obtain the modelling output of the hysteresis.

4. Experimental results

As shown in Fig. 4, the proposed modelling approach is applied to a micro-positioning stage driven by a piezoelectric actuator (PICMA P-885.30). The piezoelectric actuator has a nominal displacement of 0−10 μm and an operating voltage range from −20 to 120 V. Other experimental equipment includes a digital controller (E-712.3CD) and built-in capacitive sensors (D-015.00). The digital controller consists of a voltage amplifier (E-503.00) with 10× gain, a signal conditioner (E-509.C3A) for capacitive sensors, 16 bits A/D and 20 bits D/A converters. The capacitive sensors have a displacement resolution less than 0.5 nm. The equipment mentioned above is provided by Physik Instrumente GmbH & Co.

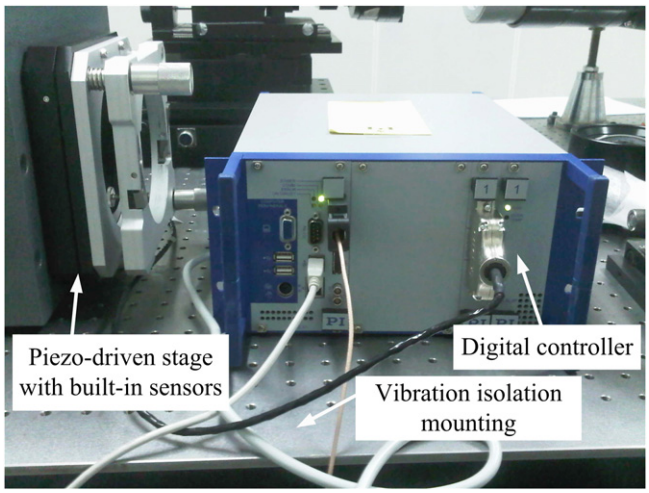

Fig. 4. Experimental setup of the piezo-driven micro-positioning system.

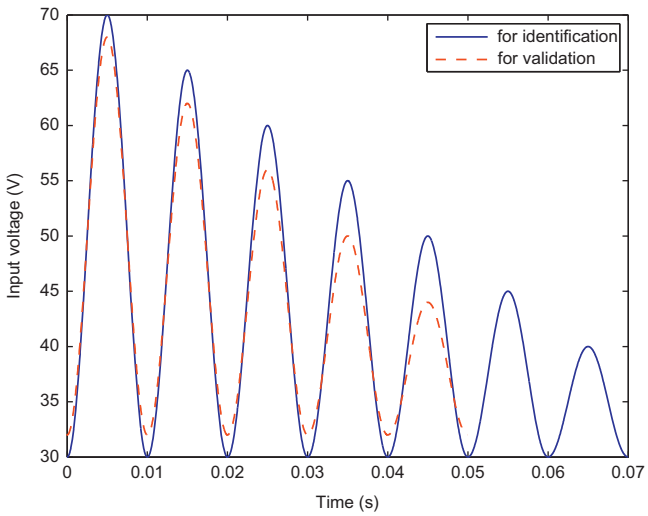

Fig. 5. The input signal for rate-independent hysteresis model identification and validation.

KG in Germany. The experiment is carried out in a laboratory with precise environmental control and its ambient temperature is kept at 22 ± 0.5 °C. All the equipment is fixed on a vibration isolation mounting. The experimental sampling frequency is selected as 50 kHz, which means that the sampling period T_s is 0.02 ms.

For convenience, we define two kinds of performance index of modelling error as follows:

$$e_r(k) = |y(k) - \hat{y}_k| / \max\{y(k), k = 1, 2, \ldots, N\} \times 100\%$$

$$e_{rms} = \sqrt{\left(\sum_{k=1}^{N} (y(k) - \hat{y}_k)^2\right) \Big/ N}$$

4.1. The experimental results on the modelling of rate-independent hysteresis in the piezoelectric actuator

The excitatory input voltage signal used for system identification and modelling is shown in Fig. 5. The signal is of sinusoidal profile with 100 Hz frequency and different amplitudes. Here 'rate-independent' means that the frequency is constant but the amplitudes can vary. Notice that the frequency chosen (100 Hz) is a value many times bigger than that usually adopted in the PI hysteresis model. We choose this value in order to validate the efficiency of the proposed model at high frequency, not just at low frequency. Due to greater influence of dynamic characteristics, the modelling of

rate-independent hysteresis at high frequency is a challenge. So, if the model is efficient at this scenario, it will be also applicable for modelling of rate-independent hysteresis at low frequency. In order to verify the generalization of the identified model, Fig. 5 also shows the excitatory input voltage signal used for model validation. It is of the same 100 Hz frequency but with distinct amplitudes from the signal used for identification.

It should be noted that the input voltages for identification and validation are different. First, we establish the hysteresis model by collecting data of the system under the excitatory input voltage for identification. Then we verify the established model's performance of generalization using another collected data of the system under the excitatory input voltage for validation.

The modelling parameters are selected as $L=6, \lambda=1, \alpha=1\times10^6$ and $\varepsilon=0$. Fig. 6 presents the model validation result of the proposed method. Fig. 7 illustrates the model validation error of the proposed method. The e_{rms} and maximum e_r are 0.0016 μm and 0.31% respectively.

For comparison, the simplified PI model proposed by Ang [9] is used to approximate the rate-independent hysteresis. The elementary operator is play operator (also referred as backlash operator). The modelling hysteresis output is a sum of weighted play operators with different thresholds and weight values. We choose 20 play operators as the elementary operators. The thresholds of the play operators are specified uniformly in [0, max $(u)/2$]. The weight values are estimated via least squares algorithm. Unfortunately, this modelling method obtains worse modelling performance and larger

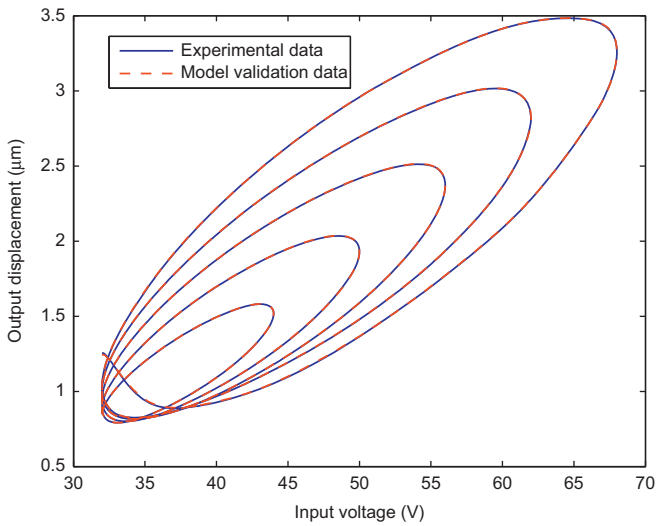

Fig. 6. The validation result of rate-independent hysteresis model.

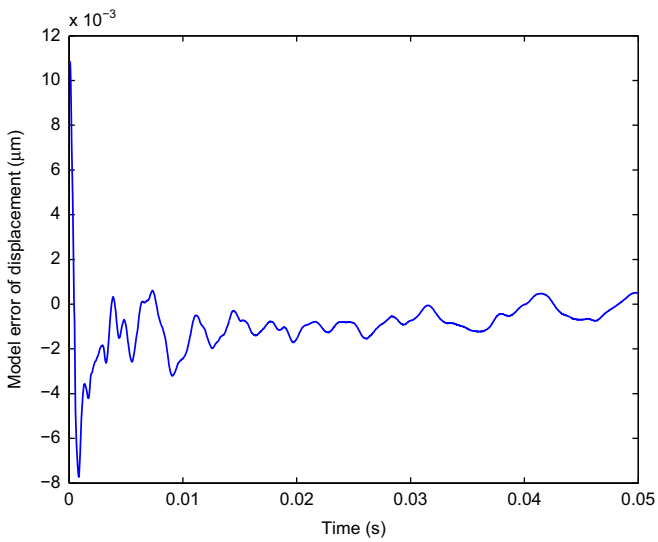

Fig. 7. The validation error of rate-independent hysteresis model.

modelling error than the proposed method of fuzzy system. The e_{rms} and maximum e_r are 0.1722 μm and 10.79% respectively. The comparison indicates that, as to rate-independent hysteresis, PI model is not efficient enough for modelling at high frequency although it is a good method for modelling at low frequency. Whereas, the proposed fuzzy system modelling method can obtain at least 1 order of magnitude better modelling performance.

4.2. The experimental results on the modelling of rate-dependent hysteresis in the piezoelectric actuator

Shown in Fig. 8, the excitatory input voltage signals used for model identification and validation are $u_{idt}(t) = 15\exp(-2t)*(\sin(120\pi*\exp(-t)*t)+1)+30$ and $u_{val}(t) = 15\exp(-2.5t)*(\sin(120\pi*\exp(-1.2t)*t)+1)+30$ respectively. Notice that the frequencies and amplitudes of the voltage signal vary as exponential functions of time.

The modelling parameters are selected as $L = 6, \lambda = 1, \alpha = 1 \times 10^6$ and $\varepsilon = 0$. Fig. 9 presents the model validation result of the proposed method. Fig. 10 illustrates the model validation error of the proposed method. The e_{rms} and maximum e_r are 0.0005 μm and 0.44% respectively.

It can be seen in Figs. 7 and 10 that the error at the beginning is large. The initial position of PZT stage does not usually correspond with the initial excitatory voltage and an initial transient dynamic response may occur. To give an overall performance of the proposed fuzzy hysteresis model, these initial data are not totally excluded for modelling and thus cause the relatively large error at the beginning.

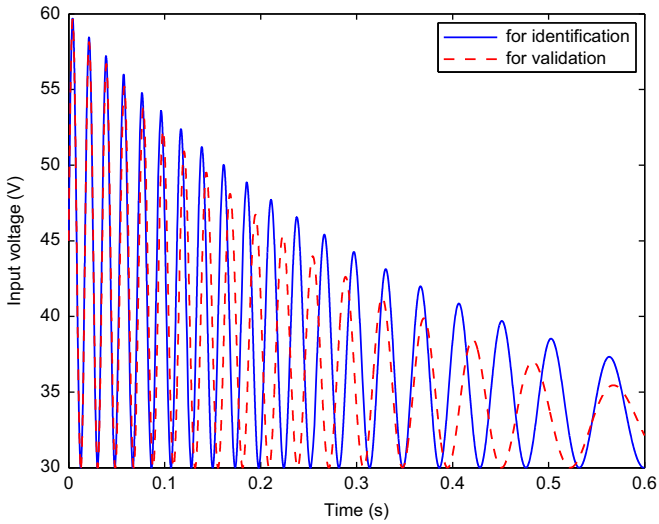

Fig. 8. The input signal for rate-dependent hysteresis model identification and validation.

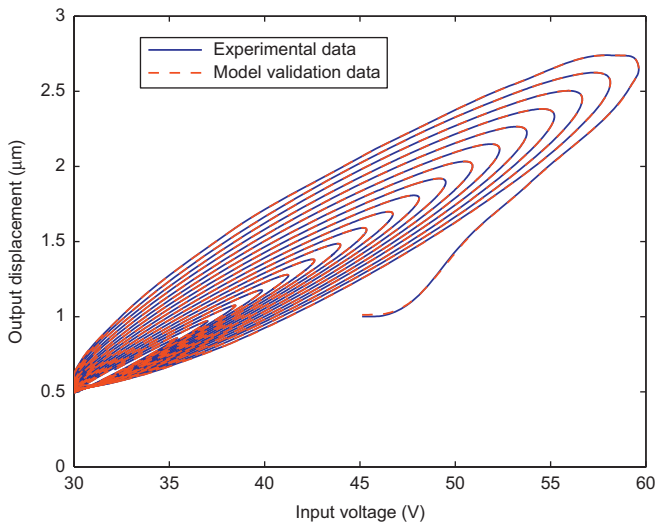

Fig. 9. The validation result of rate-dependent hysteresis model.

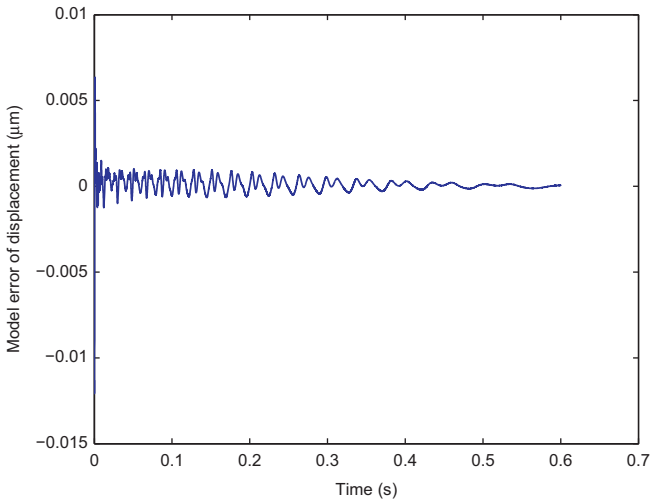

Fig. 10. The validation error of rate-dependent hysteresis model.

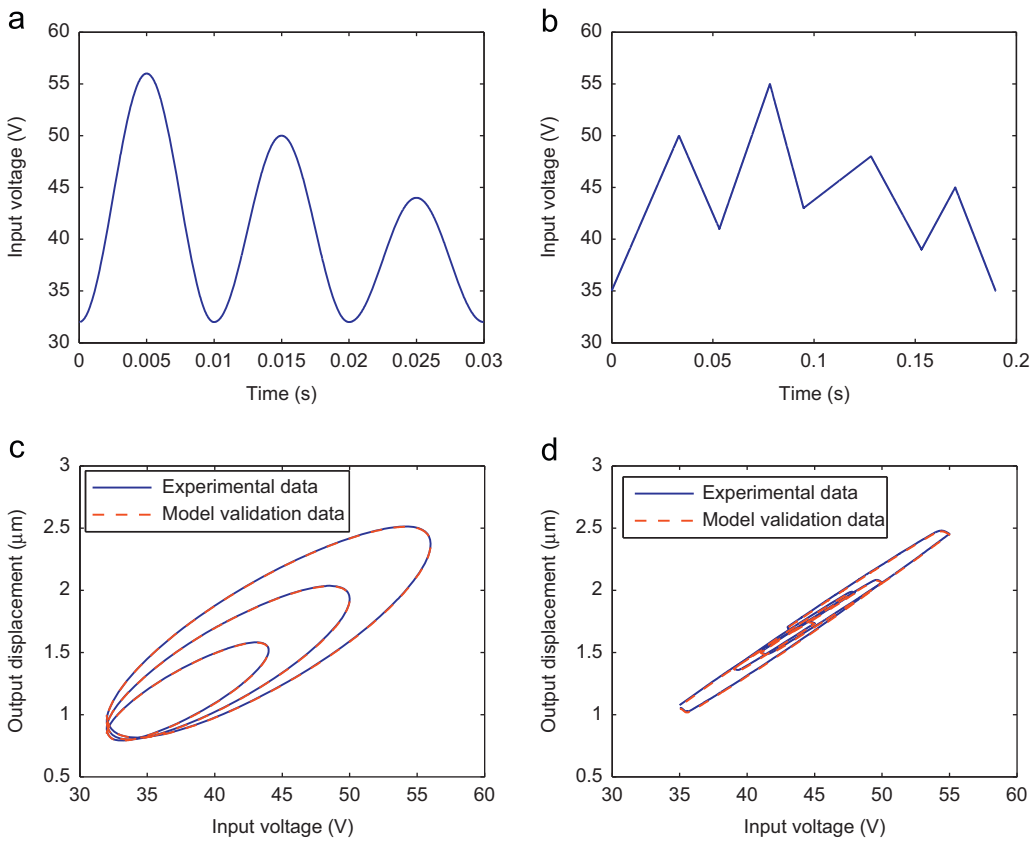

Fig. 11. The general performance of rate-dependent hysteresis model: (a) Single-frequency (100 Hz) signal; (b) non-harmonic signal; (c) the validation result under single-frequency signal and (d) the validation result under non-harmonic signal.

To validate the obtained rate-dependent model above more comprehensively, single-frequency (100 Hz) and non-harmonic signals shown in Fig. 11(a) and (b) are used to excite the PZT stage. Fig. 11(c) and (d) illustrates the modelling performance. When the 100 Hz sinusoidal signal is passed through the model, the maximum e_r is 0.15%. Regarding the non-harmonic signal, the maximum e_r of the model is 0.35%.

Compared to rate-dependent hysteresis modelling methods in the literatures by Deng [11], Ang [9] and Janaideh [10], the proposed method can obtain similar or even better modelling performance with simpler identification process.

4.3. Open-loop feed-forward control

The inverse u_{inv} of fuzzy hysteresis model can be analytically obtained as

$$u_{inv}(k) = \frac{y(k+1) - \sum_{l=1}^{L}(p^l(y_k)(q_{l1}y(k)+q_{l3}))}{\sum_{l=1}^{L}(p^l(y_k)q_{l2})}. \tag{11}$$

Shown in Fig. 12, an open-loop feed-forward controller is designed for trajectory tracking based on the inverse model of Eq. (11). In practical applications, the feed-forward controller is implemented via a 375 MHz TMS320C6748 floating-point DSP with up to 2746 million floating-point operations per second (MFLOPS). Supported by this type of hardware configuration, each control period is less than 0.02 ms.

The desire trajectory y_d is described by $y_d = 2.0 + 0.6 * \sin(2\pi * f * t)$. Here the frequencies f of y_d are chosen as 50 Hz and 100 Hz respectively. The tracking performance of the feed-forward controller is shown in Fig. 13. As to 50 Hz trajectory, Fig.13(a) illustrates the tracking result in which the tracking e_{rms} and maximum e_r are 18.6 nm and 3.14%, while Fig. 13(c) shows the compensated hysteresis result. With regard to 100 Hz trajectory, Fig. 13(b) shows the tracking result in which the tracking e_{rms} and maximum e_r are 15.2 nm and 2.91%, while Fig. 13(d) illustrates the compensated hysteresis result. A proportional feed-forward controller without the inverse model, however, can just achieve about 18% maximum tracking error. Obviously the inverse model based feed-forward controller has a good performance of trajectory tracking and hysteresis compensation. It should be noted that the model used for 50 Hz trajectory tracking is the rate-dependent model obtained in Section 4.2, while the model used for 100 Hz trajectory tracking is the rate-independent model obtained in Section 4.1.

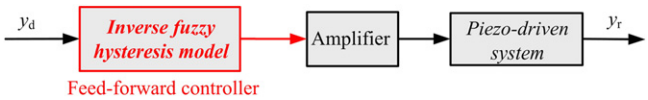

Fig. 12. Block diagram of the inverse model based feed-forward controller.

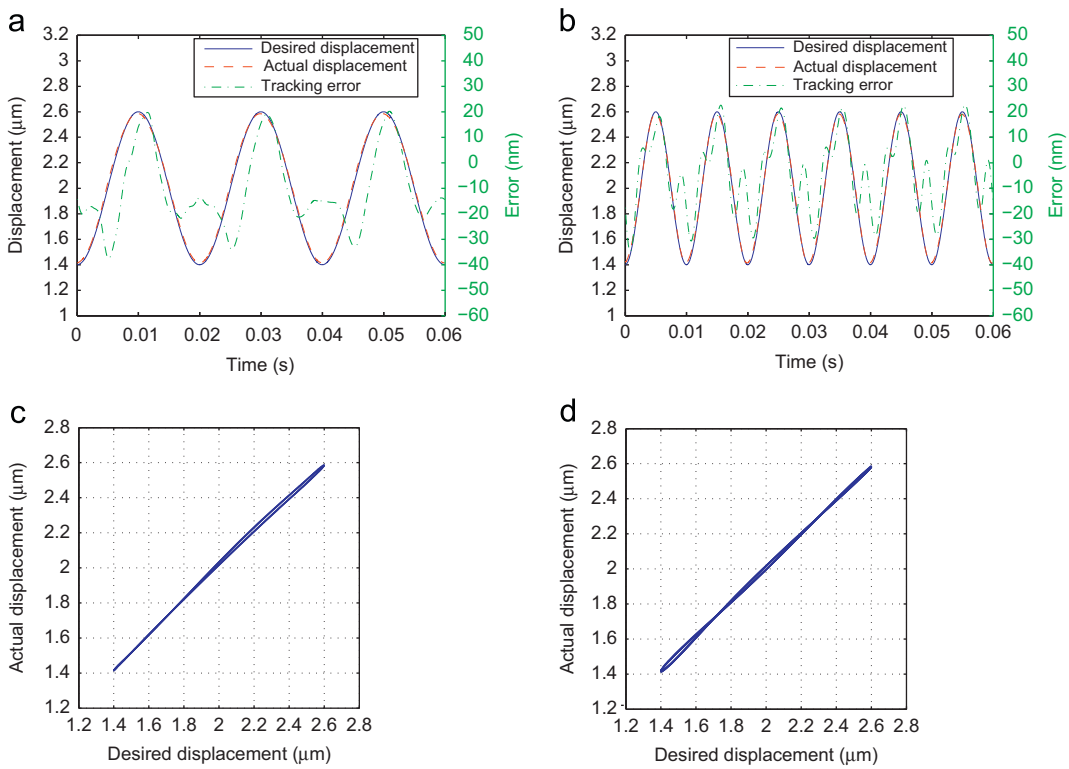

Fig. 13. The tracking performance of inverse model based feed-forward controller: (a) 50 Hz trajectory tracking result; (b) 100 Hz trajectory tracking result; (c) 50 Hz compensated hysteresis result; (d) 100 Hz compensated hysteresis result.

5. Conclusions

A fuzzy system based method is proposed in this paper for modelling hysteresis in the piezoelectric actuator. With the partial T–S fuzzy rule, the antecedent and consequent structures of the fuzzy system are identified by uniform partition and RLS algorithm respectively. Experimental results demonstrate that the model is efficient for describing both rate-independent and rate-dependent hysteresis behaviour. Besides, the inverse feed-forward controller can obviously reduce the hysteresis effects at the frequencies of 50 Hz and 100 Hz. The model has some features as follows:

(1) The inverse of the model u_{inv} can be analytically obtained, and thus an inverse model based feed-forward controller can be designed to compensate hysteretic non-linear effect.
(2) The model is simple, needs little computation time or space and moreover no other extra software such as Matlab.
(3) The model is capable of characterizing both rate-independent and rate-dependent multi-valued hysteresis precisely via introducing the extended input variables.
(4) The model can be applied on-line by obtaining the numerical range $[y_{min}, y_{max}]$ in advance.

One limitation may lie here: due to the extended input variables, hysteresis output at some time instant depends on not only hysteresis input but also hysteresis output at previous time instant.

Acknowledgments

The authors appreciate the valuable and constructive comments from the anonymous reviewers. This research is supported by the National Key Scientific and Technological Special Project of China (Grant no. 2009ZX02205).

Appendix A

This appendix lists six fuzzy rules of the fuzzy system model for rate-independent hysteresis in Section 4.1. The fuzzy set $A^l[c,\sigma]$, $l=1,2,\ldots,6$ in each fuzzy rule is characterized by membership function of $\mu_{A^l}(y_k)=\exp(-(y_k-c)^2/2(\sigma^2))$.

R^1: IF $y(k)$ is $A^1[0.6608, 0.6150]$
THEN $y(k+1)=0.6121y(k)+0.0016u(k)-0.2550$

R^2: IF $y(k)$ is $A^2[1.2758, 0.6150]$
THEN $y(k+1)=0.0696y(k)+0.0017u(k)+1.1151$

R^3: IF $y(k)$ is $A^3[1.8909, 0.6150]$
THEN $y(k+1)=0.6007y(k)+0.0015u(k)+1.1611$

R^4: IF $y(k)$ is $A^4[2.5059, 0.6150]$
THEN $y(k+1)=1.0324y(k)+0.0017u(k)-0.1756$

R^5: IF $y(k)$ is $A^5[3.1209, 0.6150]$
THEN $y(k+1)=0.8326y(k)+0.0014u(k)+0.3284$

R^6: IF $y(k)$ is $A^6[3.7359, 0.6150]$
THEN $y(k+1)=0.8733y(k)+0.0021u(k)+0.4491$

Appendix B

This appendix shows six fuzzy rules of the fuzzy system model for rate-dependent hysteresis in Section 4.2.

R^1: IF $y(k)$ is $A^1[0.4831, 0.4534]$
THEN $y(k+1)=0.8108y(k)-0.0015u(k)-0.1025$

R^2: IF $y(k)$ is $A^2[0.9365, 0.4534]$
THEN $y(k+1)=0.0226y(k)+0.0047u(k)+0.4549$

R^3: IF $y(k)$ is $A^3[1.3900, 0.4534]$
THEN $y(k+1)=-0.0123y(k)-0.0014u(k)+1.6880$

R^4: IF $y(k)$ is $A^4[1.8434, 0.4534]$
THEN $y(k+1) = 0.7710y(k) + 0.0037u(k) + 0.6780$

R^5: IF $y(k)$ is $A^5[2.2968, 0.4534]$
THEN $y(k+1) = 1.4337y(k) - 0.0005u(k) - 0.9060$

R^6: IF $y(k)$ is $A^6[2.7502, 0.4534]$
THEN $y(k+1) = 1.1658y(k) + 0.0029u(k) - 0.8047$

References

[1] PI Ceramic GmbH, Piezoelectric Ceramic Products (2005). URL 〈http://www.piceramic.com〉.
[2] S. Majima, K. Kodama, T. Hasegawa, Modeling of shape memory alloy actuator and tracking control system with the model, IEEE Trans. Control Syst. Technol. 9 (1) (2001) 54–59.
[3] I. Mayergoyz, Mathematical Models of Hysteresis and Their Applications, Elsevier, 2003.
[4] H. Janocha, K. Kuhnen, Real-time compensation of hysteresis and creep in piezoelectric actuators, Sensors Actuators: A Phys. 79 (2000) 83–89.
[5] A. Visintin, Differential Models of Hysteresis, Springer, 1994.
[6] M. Brokate, J. Sprekels, Hysteresis and Phase Transitions, Springer, 1996.
[7] M. Goldfarb, N. Celanovic, Modeling piezoelectric stack actuators for control of micromanipulation, IEEE Control Syst. Mag. 17 (3) (1997) 69–79.
[8] D. Jiles, J. Thoelke, Theory of ferromagnetic hysteresis determination of model parameters from experimental hysteresis loops, IEEE Trans. Magn. 25 (5) (1989) 3928–3930.
[9] W.T. Ang, P.K. Khosla, C.N. Riviere, Feedforward controller with inverse rate-dependent model for piezoelectric actuators in trajectory-tracking applications, IEEE/ASME Trans. Mechatronics 12 (2) (2007) 134–142.
[10] M.A. Janaideh, S. Rakheja, C.Y. Su, A generalized Prandtl–Ishlinskii model for characterizing rate-dependent hysteresis, in: The 16th IEEE International Conference on Control Applications, IEEE, Singapore, 2007, pp. 343–348.
[11] L. Deng, Y. Tan, Diagonal recurrent neural network with modified backlash operators for modeling of rate-dependent hysteresis in piezoelectric actuators, Sensors Actuators A: Phys. 148 (1) (2008) 259–270.
[12] X. Zhang, Y. Tan, M. Su, Y. Xie, Neural networks based identification and compensation of rate-dependent hysteresis in piezoelectric actuators, Physica B 405 (2010) 2687–2693.
[13] X. Zhao, Y. Tan, Modeling rate-dependent hysteresis in piezoelectric actuators using neural networks based on expanded input space method, in: The 8th IEEE International Conference on Control and Automation, IEEE, Xiamen, China, 2010, pp. 2229–2233.
[14] G. Gu, L. Zhu, Modeling of rate-dependent hysteresis in piezoelectric actuators using a family of ellipses, Sensors Actuators A: Phys. 165 (2011) 303–309.
[15] Z. Guo, J. Mao, An online intelligent modeling method for rate-dependent hysteresis nonlinearity, in: The 10th International Conference on Control, Automation, Robotics and Vision, IEEE, Hanoi, Vietnam, 2008, pp. 1458–1461.
[16] L.H. Tsoukalas, R.E. Uhrig, Fuzzy and Neural Approaches in Engineering, Wiley, 1997.
[17] L. Wang, Adaptive Fuzzy Systems and Control, Prentice Hall, 1994.
[18] L. Wang, J. Mendel, Generating fuzzy rules from numerical data with applications, IEEE Trans. Syst. Man Cybern. 22 (6) (1992) 1414–1427.
[19] J. Nie, Fuzzy control of multivariable nonlinear servomechanisms with explicit decoupling scheme, IEEE Trans. Fuzzy Syst. 5 (2) (1997) 304–311.
[20] M. Sugeno, Industrial Applications of Fuzzy Control, Elsevier, 1985.
[21] P. Li, G. Gu, L. Lai, L. Zhu, Hysteresis modeling of piezoelectric actuators using the fuzzy system, in: The 3rd International Conference on Intelligent Robotics and Applications, Lecture Notes in Artificial Intelligence, vol. 6424, Springer, Shanghai, 2010, pp. 114–124.
[22] M. Mordjaoui, M. Chabane, B. Boudjema, Dynamic magnetic hysteresis modeling with an adaptive neuro-fuzzy inference system, Int. J. Comput. Cognition 5 (2) (2007) 25–30.
[23] A. Adly, S. Abd-El-Hafiz, Efficient modeling of vector hysteresis using fuzzy inference systems, Physica B 403 (2008) 3812–3818.
[24] S. Tafazoli, M. Leduc, X. Sun, Hysteresis modeling using fuzzy subtractive clustering, Int. J. Comput. Cognition 4 (3) (2006) 15–27.
[25] W. Wang, X. Liu, Fuzzy sliding mode control for a class of piezoelectric system with a sliding mode state estimator, Mechatronics 20 (2010) 712–719.
[26] E. Mamdani, S. Assilian, An experiment in linguistic synthesis with a fuzzy logic controller, Int. J. Man-Machine Studies 7 (1) (1975) 1–13.